The Rad50 Coiled Coil Domain is indispensable for Mre11 complex functions

Marcel Hohl[1], **Youngho Kwon**[2], **Sandra Muñoz Galván**[3], **Xiaoyu Xue**[2], **Cristina Tous**[3], **Andrés Aguilera**[3], **Patrick Sung**[2], and **John H.J. Petrini**[1]

[1]Laboratory of Chromosome Biology, Memorial Sloan Kettering Cancer Center, New York, USA

[2]Yale University School of Medicine, New Haven, USA

[3]Centro Andaluz de Biología Molecular y Medicina Regenerativa, Universidad de Sevilla, Sevilla, Spain

SUMMARY

The Mre11 complex (Mre11, Rad50, Xrs2 in *S. cerevisiae*) influences diverse functions in the DNA damage response. The complex comprises the globular DNA binding domain and the Rad50 hook domain which are linked by a long and extended Rad50 coiled coil domain. In this study, *rad50* alleles encoding truncations of the coiled coil domain were constructed to determine which Mre11 complex functions required the full length of the coils. These mutations abolished telomere maintenance, meiotic DSB formation, and severely impaired HR, indicating a requirement for long range action. NHEJ, which is likely mediated by the Mre11 complex globular domain was also severely impaired by alteration of the coiled coil and hook domains, providing the first evidence of their influence on this process. These data show that Mre11 complex functions are integrated by the coiled coils of Rad50.

Keywords

DNA repair; Mre11 complex; Rad50; hook; DNA double strand break; coiled coil

INTRODUCTION

The Mre11 complex (Mre11, Rad50, Xrs2/Nbs1) plays a central role in the DNA damage response. The complex is required for double strand break (DSB) repair by homologous recombination (HR) and non-homologous end joining (NHEJ), cell cycle checkpoint activation, telomere maintenance and meiotic recombination [1]. These diverse functions reflect the diverse activities specified by the complex, which include DNA bridging, mediated primarily by Rad50, and nuclease activity specified by Mre11 [2,3]. A structural role for the Mre11 complex in HR was suggested by the observation that *mre11Δ* and *rad50Δ* mutations, unlike nuclease dead *mre11* alleles, acutely impaired spontaneous and induced HR between sister chromatids while increasing spontaneous interhomolog recombination [4–7].

Structural analysis of Rad50 suggested a mechanistic basis for the Mre11 complex's promotion of sister chromatid recombination. A conserved "hook" motif at the center of the coiled coil domain contains two invariant cysteines (CXXC), which in combination with a second Rad50 protomer coordinates a zinc ion to form an interaction interface between Mre11 complexes [8]. The geometry specified by this interface readily accommodates a model in which Mre11 complex dimers bridge DNA molecules such as sister chromatids during HR (Fig. 1a) [9]. Replacement of the hook domain with a ligand–inducible dimerization cassette demonstrated that Mre11 complex tethering via Rad50 was critical for DSB repair, supporting the model suggested by structural information. Loss of hook function also impaired telomere maintenance and meiotic DSB formation [10], demonstrating that the hook's function extends beyond DNA repair.

The Rad50 coiled coil domain in *Saccharomyces cerevisiae* consists of roughly 900 residues that separate the Walker A and B ATPase domains. The coiled coils fold back on themselves in an antiparallel manner to bring the Walker A and B domains together with the CXXC motif of hook domain at the distal apex. The ATPase is within the globular domain, a heterotetrameric assembly containing dimer interfaces between two Rad50 Walker A and B motifs and between two Mre11 molecules [11]. These interfaces comprise the DNA binding and nuclease domains of the complex (Fig. 1a), and structural data suggests a model wherein the globular domain situates DNA ends to promote NHEJ [12]. The coiled coils are conserved in all known Rad50 orthologs as well as in members of the SMC protein family. In the structure predicted for the eukaryotic Mre11 complex, the fully extended Rad50 coiled coil domain could span hundreds of angstroms in the hook–mediated dimerization state [1,13]. The basis for this apparent length requirement, and whether all of the various Mre11 complex functions require such a vast distance are not clear.

Atomic force microscopy studies revealed that DNA binding induced the Rad50 coiled coil arms to adopt a configuration favorable for the hook-hook interaction [14]. In addition, several studies demonstrated that the Mre11 complex was capable of binding and tethering DSB ends *in vitro* [15–20]. Collectively, these data support a model wherein the Mre11 complex effects DNA assemblies that are favorable for homology directed recombinational DNA repair through the concerted action of the hook and coiled coil domains.

Mutations affecting the conserved cysteine residues of the hook domain disrupt Mre11 complex integrity [8], suggesting a conformational crosstalk between the hook and the Rad50 globular domain. We tested the hypothesis that the functions mediated by the distal globular and hook domains of the Mre11 complex are integrated by the extended coiled coils of Rad50. Two classes of *S. cerevisiae rad50* mutants were derived, *rad50^{2TEV}* and *rad50^{coils}*. In cells expressing the *rad50^{2TEV}* allele, the hook domain can be removed acutely *in vivo* from an otherwise normal Rad50 upon expression of the TEV protease. In *rad50^{coils}* mutants, a TEV-cleavable hook domain is appended to progressively shortened coiled coil domains.

We found that truncation of the Rad50 coiled coil domain abolished meiotic DSB formation and telomere length maintenance. Although most truncations also abolished HR, the *rad50^{sc+h}* allele in which 243 residues were excised from the coiled coils retained substantial HR functionality that was completely dependent upon the hook domain. Remarkably, NHEJ was also severely impaired by coiled coil truncation, and loss of the hook domain had a marked effect on the structure of NHEJ repair junctions after HO cleavage on the chromosome. The data thus show that the HR and NHEJ functions of the complex can be separated, and suggest that the hook and coiled coil domains influence the DNA binding domain to promote NHEJ.

RESULTS

Rad50 coiled coil mutants

In this study, we sought to examine the functional relationship between the Rad50 hook and coiled coil domains, which links the hook domain to the globular domain at which Mre11, Rad50 and Xrs2 assemble and DNA is bound [1]. Two classes of *rad50* mutants were analyzed. The *rad50^{2TEV}* allele allows the hook domain to be acutely removed from an otherwise normal Rad50 upon expression of the TEV protease. In the second class of mutants, a TEV–cleavable hook domain is appended to progressively shortened coiled coil domains (Fig. 1b).

Previously, we created a "hookless" *rad50* mutant strain (*rad50^{hook}*) in which Rad50 is encoded in halves, one from each of two alleles lacking the residues that comprise the hook. The *rad50^{hook}* phenocopied complete Mre11 complex deficiency [10], providing a proof-of-principle that the Rad50 hook was required for Mre11 complex function. However, Mre11 complex assembly was not sufficiently robust in that setting for detailed molecular analysis. The new system presented here circumvents this limitation, and allows direct assessment of hook functions in conjunction with those of the coiled coil domain.

In the *rad50^{2TEV}* gene product, two TEV protease cleavage sites (ENLYFQG) were inserted in tandem (*2TEV*) on either side of the hook domain at codons 573 and 829 (*rad50^{2TEV573/829}*, hereafter *rad50^{2TEV}*). Those positions are not predicted to be coiled coils and correspond to a segment of the human Rad50 protein exhibiting increased flexibility [21]. The *2TEV* insertions on either side of the hook are predicted to appose one another within the associated N and C terminal anti-parallel coiled coil segments of Rad50 (Fig. 1b).

In the various coiled coil truncation mutants, the central 28 amino acids of the hook motif (ALEIAERDSC**C**YL**C**SRKFENESFKSKLL; the zinc-binding cysteines are bold underlined) were appended to increasingly shortened coiled coils at the distal end. The smallest deletion reduces the length of the coiled coil by 234 amino acids, 105 and 129 amino acids for each side, either with the minimal hook domain in *rad50^{sc+h}* (*short coil +hook, sc+h*) or without in *rad50^{sc}* (*short coil, sc*). Virtually identical Rad50 protein fragments are produced upon TEV induction in *rad50^{2TEV}, rad50^{sc}* and *rad50^{sc+h}* (Fig. 1b), differing only in the amino acids flanking the TEV cleavage sites. Larger coiled coil truncation mutants containing the minimal hook lack residues 394–678 and 705–960 in *rad50^{vsc+h}* (*very short coil+hook, vsc+h*) and 229–678 and 705–1120 in *rad50^{nc+h}* (*no coil +hook, nc+h*; Fig. 1b).

Induced loss of the Rad50 hook domain by TEV cleavage *in vivo*

The *rad50^{2TEV}* allele was integrated at the native *RAD50* locus in a galactose inducible TEV protease expressing strain [22]. Expression of the TEV protease was detectable within 30 minutes after galactose addition, and the appearance of distinct Rad50^{2TEV} cleavage fragments was maximal by four hours (Fig. 1c, 1d and 1f). Efficient TEV cleavage of Rad50^{2TEV} proteins with TEV cleavage sites on one side of the hook (*2TEV573* or *2TEV829*) was also confirmed by incubation of Rad50–immunoprecipitates with recombinant TEV protease (Fig. 1e).

Mre11 complex integrity and DNA association

Mre11 complex integrity is required for most if not all of its function, indicating that the individual components do not specify autonomous activities outside of the complex. To assess whether Mre11 complex integrity was compromised by insertion of two 2TEV sites, Mre11 complexes containing WT or Rad50^{2TEV} were assembled with purified Mre11 and

Xrs2, and separated by gel filtration. The stoichiometry of the Mre11 complex with Rad50^{2TEV} was similar to that of the wild type complex (Fig. 2a).

Next we examined whether TEV–induced cleavage of the Rad50 hook domain affects the Rad50–Mre11 interaction. Rad50 WT, Rad50^{2TEV} and TEV-treated Rad50^{2TEV} were incubated with His-tagged Mre11, and protein complexes were captured on nickel-beads. Rad50 WT and full length Rad50^{2TEV} coeluted with His-tagged Mre11, demonstrating that Rad50^{2TEV} associates stably with Mre11 (Fig. 2b, on the left). Rad50^{2TEV} cleavage fragments (f1 and f3) also co-eluted with Mre11-his$_6$ (Fig. 2b, on the right), indicating that the Mre11 complex remains intact after TEV–mediated cleavage of the Rad50 hook.

Mre11 complex integrity in *rad50* coiled coil mutants was assessed by co–immunoprecipitation from extracts of cells containing N-terminal 8xFlag-tagged Mre11 and C-terminal 3xHA-tagged Rad50 (Fig. 2c). Immunoprecipitation with FLAG antisera recovered Rad50 WT, Rad50^{sc}, Rad50^{sc+h} and Rad50^{vsc+h} proteins from FLAG-Mre11 expressing strains, but not from cells expressing untagged Mre11. In contrast, the Rad50^{nc+h} protein, in which almost the entire coiled coil domain was deleted, was not recovered in FLAG immunoprecipitates.

These data demonstrate that the hook and majority of the coiled coils are not required for the Rad50-Mre11 interaction, and place the Mre11 interaction site on Rad50 proximal to the Walker A and B domains similar as in the archaeal Mre11 complex, and consistent with previous studies [14,16,23,24]. Recent structural analyses of two archeal and a bacteria species place the Mre11-Rad50 interaction interface within the first ≈ 6 heptad repeats of the coiled coil proximal to the ATPase core [25–27]. These coiled coil residues are present in the Rad50^{nc+h} protein (Δ229–678 and Δ705–1120), yet Mre11 interaction is abolished, suggesting that the residual coiled coil may be structurally perturbed in this mutant.

Yeast two-hybrid assays also indicate that the Mre11 complex integrity is unaffected in all coiled coil mutants except in *rad50^{nc+h}* (Supplementary Fig. 3d). These data suggest that Mre11 complex is intact following acute removal of the hook domain, and that complex integrity is not compromised by removal of coiled coil residues proximal to the hook domain.

We assessed the DNA binding capacity of Rad50^{2TEV} protein and Rad50^{2TEV}-containing Mre11 complexes using electrophoretic mobility shift assays (EMSA). TEV cleavage had no effect on DNA binding of Rad50^{2TEV} protein and Mre11 complexes, demonstrating the Rad50 and Mre11 complex DNA association does not require the hook (Fig. 2d and Supplementary Fig. 1). As shown previously with WT Rad50 [18], DNA binding of Rad50^{2TEV} protein was ATP-dependent irrespective of TEV cleavage (Fig. 2d, lane 6). As ATP binding promotes dimerization of the Rad50 Walker A and B ATPase domains [28], the data indicate that the Rad50 homodimerization via the globular domain is hook-independent.

Meiosis and telomere maintenance

Having established the integrity and proficiency of Mre11 complexes containing structural variants of Rad50 to bind DNA, we assessed the functionality of these mutants *in vivo*. Previous analyses suggested that the Rad50 hook domain was required for meiotic DSB formation and telomere maintenance [10].

To assess the ability of Rad50 variants to initiate meiotic recombination, homozygous diploid SK1 cells were sporulated and spore viability was assessed. Virtually all spores of *rad50^{sc+h}* as well as of *rad50^{sc}* and *rad50^{vsc+h}* were inviable among more than 30 tetrads tested (data not shown). DAPI staining of tetrads in all *rad50^{coils}* mutants suggested aberrant

chromatin segregation, reminiscent of *rad50Δ* or *spo11Δ* cells in which DSBs are not formed (Fig. 3a and data not shown). Accordingly, *rad50^coils^* spore lethality was associated with a failure to induce meiotic DSBs. Sae2-proficient or –deficient cells were cultivated for 0, 4, 8 and 12 hours in sporulation media and DSB formation at the *HIS4-LEU2* hotspot was assessed (Fig. 3b). In *sae2Δ* cells, Spo11-bound double-strand breaks (DSBs) accumulate [29], allowing detection of unresected DSBs by Southern blotting. No meiotic DSBs were detectable in *rad50^sc+h^*, *rad50^sc^* or *rad50^vsc+h^ sae2Δ* double mutants (Fig. 3b and data not shown).

We next examined telomere lengths in the Rad50 variants. Freshly dissected spores of heterozygote diploids (*rad50/WT*) were grown for 60 generations and telomere length was determined by Southern blotting. As the *rad50^sc+h^* mutant exhibited partial cold sensitivity in various aspects (Supplementary Fig. 3 and Supplementary Fig. 4a), telomere length was assessed following propagation at 30°C and 23°C. As for meiotic DBS formation, all *rad50^coils^* mutants phenocopied *rad50Δ* with respect to telomere length irrespective of temperature (Fig. 3c).

A modicum of telomere function was retained in *rad50^sc+h^* (Supplementary Fig. 2d). The plating efficiency of *rad50^sc+h^* was similar to *WT* after 50 generations (87% versus 101%; Fig. 3d). Decreased telomere length was also noted in *rad50^2TEV^* cells upon TEV expression, however the effect was difficult to interpret as hook cleavage was not complete over prolonged incubation in galactose media (Supplementary Fig. 2b and Supplementary Fig. 2c). The data show that although variant complexes were physically intact, reduction in the length the coiled-coils rendered them defective in promoting meiotic DSB formation and telomere maintenance.

Acute Rad50 hook loss and coiled coil shortening

The functionality of Mre11 complex variants in DNA repair was subsequently addressed. *WT*, *rad50Δ* and *rad50^2TEV^* cells were spotted on galactose plates to induce TEV expression, with or without MMS (Fig. 4, top panel). Cells expressing single *2TEV573* and *2TEV829* insertions were also included. In the absence of TEV induction, the survival of *rad50^2TEV^* cells on MMS was indistinguishable from *WT*. TEV-mediated cleavage of the hook in *rad50^2TEV^* cells resulted in MMS sensitivity, which was slightly less pronounced than *rad50Δ* (Fig. 4, top right panel). Strains in which 2*TEV* sites were inserted at a single position (*573* or *829*) did not exhibit MMS sensitivity upon TEV induction, although TEV cleavage was efficient in these proteins (Fig. 1e and data not shown). The *rad50^sc^* mutant, which expressed a protein product virtually identical to that produced by TEV-mediated cleavage of Rad50^2TEV^, was indistinguishable from *rad50Δ* (Fig. 4), indicating that incomplete cleavage of Rad50^2TEV^ likelyaccounts for the MMS resistance in *rad50^2TEV^*. Supporting this view, a small amount of uncleaved Rad50^2TEV^ was evident even after prolonged TEV induction (Supplementary Fig. 2c). Similar results were obtained after acute MMS treatment (Supplementary Fig. 3a).

*rad50^vsc+h^* and *rad50^nc+h^* phenocopied *rad50Δ* irrespective of TEV induction. *rad50^sc+h^* was nearly as MMS resistant as *WT* on glucose-containing MMS media, but survival was reduced to the levels of *rad50^sc^* and *rad50Δ* upon TEV induction (Fig. 4 and Supplementary Fig. 3a).

Sister chromatid recombination is promoted by the Rad50 hook

In *S. cerevisiae*, DSBs are predominantly repaired by homologous recombination between sister chromatids [30]. Hence the MMS sensitivity caused by cleavage of the hook domain and coiled coil truncation likely reflects impaired sister chromatid recombination (SCR). To

directly test the idea that the Rad50 hook promotes intersister recombination, we used a plasmid-based SCR assay [7,31]. In this system, HO endonuclease creates a nick at an incomplete HO site on the *pTINV* recombination substrate. The nick gives rise to a DSB during DNA replication on one of the two plasmid sister chromatids formed. The HO site lies in one of two *leu2* repeats, such that a novel restriction fragment is created by recombination between the repeats. SCR is then detected by Southern blotting of plasmid DNA with a *LEU2* probe (Fig. 5a).

Concomitant induction of HO endonuclease and TEV protease was carried out in strains containing both *GAL-HO* and *GAL-TEV*, or *GAL-HO* alone. $rad50^{2TEV}$ exhibited *WT* levels of SCR in *GAL-HO* strains over a 6 hr time course (Fig. 5b, top). In *TEV*-expressing $rad50^{2TEV}$ cells, SCR repair products were undetectable up to 4 hrs, with a slight accumulation by 6 hrs. Consistent with the MMS resistance of $rad50^{sc+h}$, SCR products accumulated, albeit more slowly than in *WT*, whereas $rad50^{sc}$ and $rad50^{vsc+h}$ cells phenocopied $rad50\Delta$ cells (Fig. 5b, bottom and data not shown). These data provide direct physical evidence that the Rad50 hook domain promotes SCR, and further that efficient SCR can be effected when the Rad50 coiled coil domain is shortened.

Mre11 complex deficiency increases the rate of heteroallelic recombination in vegetatively growing cells [5,32]. We hypothesize that Rad50 hook-mediated bridging channels DSB repair to the sister chromatid and away from the homolog as a repair template. Spontaneous mitotic heteroallelic recombination was measured in diploids containing two *ade2* heteroalleles, *ade2-n* and *ade2-ISceI* [33,34] in which gene conversion to restore a functional *ADE2* gene cause white sectoring in otherwise red colonies (see Fig. 5c, photograph on the left). Most *WT* and $rad50^{2TEV}$ colonies showed only 0–2 sectors (Average 1.0 sectors per colony), whereas $rad50\Delta$, $rad50^{sc}$, and $rad50^{vsc+h}$ showed in average more than 10 white sectors per colony. TEV induction increased sectoring in $rad50^{2TEV}$ approximately 3–4 fold to 3.7 sectors per colony (Fig. 5c). $rad50^{sc+h}$ exhibited an intermediate level of sectoring that was increased to $rad50\Delta$ levels upon hook removal (see photographs in Supplementary Fig. 4b). These data support the view that the sister chromatid bridging by the Rad50 hook domain suppresses interhomolog recombination.

Separation of HR and NHEJ functions

The Mre11 complex also participates in NHEJ [15,35–37]. Recent structural studies provide evidence for a short range DNA tethering via dimerization of Mre11 within the globular domain of the Mre11 complex, which might influence NHEJ [12]. Previous data suggest that Mre11 complex-mediated NHEJ occurs primarily outside of G1, and therefore may take place in presence of a sister chromatid [35]. This observation raised the possibility that long range bridging mediated by the Rad50 coils and the hook could influence NHEJ.

To test this prediction, *WT*, $rad50\Delta$ and $rad50^{coils}$ mutant cells were transformed with either EcoRI (5′ overhang) or SacI (3′ overhang) cut plasmid substrates and the NHEJ efficiencies were calculated from the ratio of transformants obtained with cut versus uncut plasmid (Fig. 6a). Contrary to our expectation, the $rad50^{coils}$ mutants were severely impaired in plasmid rejoining. In contrast to its HR phenotype, $rad50^{sc+h}$ was only marginally (3-fold) better than $rad50\Delta$ at plasmid reclosure. Residual NHEJ function in $rad50^{sc+h}$ may partially reflect a role of the hook domain, as $rad50^{sc}$ was more severely impaired than $rad50^{sc+h}$.

NHEJ on the chromosome was assessed at an HO induced DSB at the *MAT* locus [35]. In this setting, chronic expression of the HO endonuclease selects for inactivation of the HO site through Pol4-dependent addition (+CA; predominant in *WT* cells) or Pol2-dependent loss (ΔACA or ΔCA; predominant in $rad50\Delta$) [35,38]. In $rad50\Delta$ cells, the level of survival was 0.002%, 115-fold less than *WT* (Fig. 6b). As in the plasmid-based assay, chromosomal

NHEJ was defective in *rad50^{coils}* mutants. Survival frequencies in *rad50^{sc+h}* and *rad50^{sc}* mutants were only slightly higher than *rad50Δ*, 5.4-fold (*rad50^{sc}*) and 5.6-fold (*rad50^{sc+h}*), respectively. In all cases, the sequences at the repair junctions bore the Δ(A)CA signature seen in *rad50Δ* survivors (Fig. 6b and Supplementary Fig. 5a).

Whereas truncation of the coils caused NHEJ defects, TEV expression in *rad50^{2TEV}* cells did not compromise viability, suggesting that bridging by the hook is not required for NHEJ (Fig. 6c). However, TEV-mediated ablation of the hook alters the structure of the HO junctions. Whereas in the absence of TEV, *rad50^{2TEV}* survivors harbored *WT* insertions (mostly +CA and +ACA events), TEV expression in *rad50^{2TEV}* cells resulted in a marked shift towards the *rad50Δ* deletion signature (Fig. 6c, bottom and Supplementary Fig. 5c). Hence, TEV cleavage of Rad50^{2TEV} influences the imprecision of NHEJ, but does not appear to compromise the joining step of the reaction.

Short term, as opposed to chronic induction of HO endonuclease provides an assessment of chromosomal NHEJ that is not confounded by selection for loss of the HO site. *rad50^{coils}* cells were cultured in galactose containing media for 2 hours to express HO throughout the cell cycle, and HO expression was suppressed by addition of glucose. DNA was prepared at 1.5, 3 and 5 hours after HO suppression, and resealing of the HO site was measured by quantitative PCR (Fig. 6d). At five hours in glucose, 23.6% of *WT* and 7.1% of *rad50^{sc+h}* cells repaired the HO DSB, whereas DSBs persisted in *rad50Δ* and *rad50^{sc}* cells and were apparently degraded as QPCR signals decreased over the course of the experiment (−3.4% and −2.8%, respectively). The *rad50^{sc+h}* residual NHEJ activity again suggests that the hook domain may contribute to NHEJ. Consistent with the quantitative PCR results, cell survival after 2 hours HO induction was markedly better for *rad50^{sc+h}* (4.7%) than *rad50^{sc}* and *rad50Δ* (both 1.2%, Fig. 6e). Collectively, these data suggest that the distal (i.e., hook and coiled coil) domains of the Mre11 complex affect NHEJ, but in a manner largely independent of the Rad50 hook domain. These observations suggest that the phenotypes observed in *rad50^{coils}* and *rad50^{2TEV}* may be attributable to changes in the disposition of DNA ends in the globular domain.

Discussion

Genetic, physical and biochemical evidence support a model in which Mre11 complex homodimerization via the Rad50 hook domain promotes homologous recombination [15–19]. To test this model, we designed the *rad50^{2TEV}* mutation in which the hook domain can be removed acutely *in vivo* upon expression of the TEV protease. In *rad50^{coils}*, hook removal from progressively truncated coiled coils can be effected similarly. We reasoned that *rad50^{2TEV}* and *rad50^{coils}* (Fig. 1b) would provide separation of hook functions from those of the coils. The coils are a conserved feature among Rad50 orthologs [13], yet their significance for the functions of the Mre11 complex is not well understood.

The formation of Spo11-induced DSBs and the maintenance of telomeres was abolished in the *rad50^{coils}* mutants. These observations argue that the Mre11 complex promotes these functions over a distance requiring the full extent of the coiled coil domain. It is conceivable that the relative intolerance of Mre11 complex functions to coiled coil truncation reflects the state of the sister chromatids when those functions are executed. For example, the distance separating the sisters in proximity to the replication fork (at DSBs formed in the SCR assay) may be shorter than at sites destined for Spo11 cleavage or at telomeres. However, Spo11 cleavage is not impaired in meiotic cells in which DNA replication is blocked and sister chromatids are absent [39]. Moreover, we have not demonstrated that the loss of intersister bridging *per se* underlies the loss of telomere maintenance. It is thus equally likely that the

coiled coils and the hook are also required to mediate long range interactions unrelated to intersister bridging.

Contrary to our expectations, the coiled coil mutants were severely impaired in NHEJ. As HR functions are largely intact in $rad50^{sc+h}$, these data demonstrate that HR and NHEJ functions of the complex are separable. NHEJ was also affected by ablation of the hook domain. HO induction did not compromise viability of $rad50^{2TEV}$ cells, yet the majority of HO junctions bore the ΔCA/ACA signature typical of $rad50\Delta$ (Fig. 6c). The survival of $rad50^{2TEV}$ is unlikely to reflect inefficient cleavage, as chronic HO induction in strains having a single TEV insertion on one side of the hook were unaffected (data not shown). TEV cleavage of Rad50^{2TEV} produces a protein identical to Rad50^{sc}; hence Rad50^{2TEV} molecules that are cleaved prior to DNA binding are likely to behave as Rad50^{sc}. The difference in survival between $rad50^{2TEV}$ and $rad50^{sc}$ likely reflects that most Rad50^{2TEV} molecules are cleaved *after* Rad50^{2TEV} binds DNA and alters the disposition of the globular domain.

How do the distal Rad50 domains influence NHEJ? Previous studies have suggested that Rad50 deficiency in *S. cerevisiae* primarily influences NHEJ in S and G2 cells [35]. The observation that the coils and the hook domain influence NHEJ raise the possibility that Mre11 complex-mediated long range interactions are required for both HR and NHEJ pathways. However, the efficiency of NHEJ was unaffected upon cleavage of Rad50^{2TEV} (Fig. 6c). Therefore, we favor the interpretation that the cell cycle specificity of Mre11 complex NHEJ activity is more likely attributable to differences in the activities or abundance of other NHEJ components [40].

The heterotetrameric (two Rad50 and two Mre11) globular domain houses the complex's DNA binding domain, which comprises residues from both Mre11 and Rad50 [1, 25–27]. Recent structural data suggest that the globular domain bridges DNA ends held within it in a manner that would promote NHEJ [12]. Accordingly, we propose that the phenotypic outcomes observed upon coiled coil truncation and/or hook domain ablation may be attributed to two nonexclusive effects on the disposition of DNA ends within the globular domain that may also impair higher order assembly (Fig. 7).

First, alterations in the coiled coil domains or ablation of the hook may cause axial rotations that are transduced into the globular domain that may alter the disposition of DNA ends within it. Coexpression of $rad50^{sc+h}$ and a $rad50$ allele containing an insertion of coils (*long coil+hook*) failed to rescue the telomere maintenance defect of $rad50^{sc+h}$ (data not shown), indicating that the effects of the coiled coil truncations are not simply reflective of a distance requirement.

Second, in addition to its length, the presence and relative location of flexible regions within the coiled coil domains is conserved among Rad50 orthologs [13]. Removal of segments within the coiled-coils may alter the flexible regions and compromise function. This speculative model would predict that truncations of the coils and removal of the hook would alter the structure of both the coiled coil and globular domains (Fig. 7). Finally, it is also possible that coiled coil mutations impair protein-protein interactions required for NHEJ and other DNA metabolic processes. Previously reported two hybrid interactions between Mre11 and Hdf2 as well as Xrs2 and Lif1 [41,42] were intact in $rad50^{sc+h}$ and $rad50^{vsc+h}$, whereas the interaction was impaired in $rad50^{sc}$ and $rad50^{nc+h}$ as in $rad50\Delta$ (data not shown), leaving the possibility of an as yet undescribed interaction between the Mre11 complex and other NHEJ factors open.

This conception resonates with recent structural information regarding archeal Mre11-Rad50 complexes. Those data indicate that the Rad50 ATPase domain influences the organization

of the Mre11 catalytic domain, and further that changes within those components of the globular domain alter the disposition of the coiled coils [25–27]. In essence, we propose that the converse occurs in the coiled coil mutants: alterations in these distal domains alter the disposition of the globular domain to impair NHEJ (Fig. 7). Supporting an effect on the catalytic domain itself, DSB end resection was delayed in *rad50^{sc}* to the same extent as in *rad50Δ* G2 arrested cells. As with NHEJ, end resection was marginally restored in *rad50^{sc+h}* (Supplementary Fig. 6).

It is clear from this study that despite the large distances separating them, the hook and coiled coil domains of Rad50 strongly influence events transpiring at the Mre11 complex globular domain. The non-modular behavior of the Mre11 complex likely holds the key(s) to the regulation of its diverse functions in the DNA damage response.

METHODS

Yeast Strains and media

Strains used were in the W303 (*RAD5),* DBY745 or SK1 background (Supplementary Table 1). Site-directed mutagenesis was done using a single mutant primer [43] and KOD HiFi polymerase (Novagen). Details of strain and plasmid constructions are available upon request. Transformations were performed using the standard transformation protocol [44]. Strains containing the *GAL–TEV–myc::TRP1* construct [22] were grown in synthetic media without tryptophan, or in absence of *GAL–TEV* in complete media. Cells were grown in media containing 2.6% glycerol, 2.6% ethanol and 1% succinate, re-diluted to 10^6 cells ml^{-1} in 2% lactate media and grown to 1×10^7 cells ml^{-1} prior addition of 1/10 volume of 20% galactose (Sigma, G0750). Galactose induction on plates was done by plating cells grown in lactic acid media on glycerol-ethanol plates (see above) containing 2% galactose. Cells were plated in duplicate in colony forming assays. All experiments were performed at least three times, unless stated otherwise.

Damage sensitivity assays

Five-fold serial cell dilutions (250,000 - 80 cells per spot) were spotted on plates without or with S-phase clastogens and incubated for 3 days at 30°C, 4 days at 23°C and 2 days at 37°C.

Immunoprecipitations and Western blot

Yeast cell extracts were prepared as described [45]. Immunoprecipitations were done with protein A/G Sepharose (Callbiochem) pre-blocked with 5% BSA, 2 mg cell extracts and 2–5 μg rabbit anti-Rad50 (#64911), rabbit FLAG M2 (Sigma F7425) or rabbit anti-HA (Bethyl, A190–108A) antisera. Western blotting was performed using rabbit anti-Rad50 (#64911) or rabbit anti-Mre11 (#59567) antisera [51] or mouse anti-HA (12CA5; Roche).

Purification of WT and Rad50^{2TEV} proteins and Mre11 complexes

Rad50, Mre11, and Xrs2 proteins were purified as published [18]. Rad50^{2TEV} was expressed in a *rad50Δ*–derivative of strain BJ5464 carrying *pPM231-rad50^{2TEV}* and purified as described for WT Rad50 [46]. His$_6$-Mre11 protein expression was induced with 0.5 mM IPTG (4 h, 37 °C) in BL21 (DE3) pLysS cells (Novagen) transformed with *pRSET-His$_6$-MRE11* [47] and purified by Ni-NTA agarose (Qiagen), Macro-hydroxyapatite (Bio-Rad), SP-Sepharose fast flow (Amersham Biosciences), and Mono-Q (Amersham Biosciences). Mre11 complexes containing WT Rad50 or Rad50^{2TEV} were assembled as described [15] and purified by Superose 6 PC 3.2/30 size exclusion column. TEV cleavage of Rad50^{2TEV} (1:10 enzyme to substrate ratio) was performed for 4 hours at 4°C in T-500 buffer (25 mM Tris-HCl, pH 7.5, 500 mM KCl, 10% glycerol, 0.5 mM EDTA, 0.01% Igepal, 1 mM DTT).

To assess the Mre11–Rad50 interaction, WT Rad50, Rad50^{2TEV}, and TEV protease treated Rad50^{2TEV} (4 μg each) were incubated at 4°C for 30 min with His$_6$-Mre11 (2 μg) in T-150 buffer (see above, 150 mM KCl) containing 10 mM imidazole and then for another hour in presence of Ni-NTA agarose. The beads were washed (4x) with 200 μl of T-150 buffer and boiled in Lämmli buffer and fractions (supernatant, wash, eluate) were run on a 10% SDS-PAGE.

Electrophoretic mobility shift assay

WT or Rad50^{2TEV} proteins (0–200 nM) were incubated with 10 nM ^{32}P-labeled 83-bp double stranded DNA substrate [18] in 10 μl of DNA binding buffer (30 mM Tris-HCl, pH 7.5, 100 μg ml^{-1} BSA, 5 mM MgCl$_2$, 50 mM KCl, 2 mM ATP, and 1 mM DTT). After 10 min incubation at 37°C, samples were loaded on a 5% native polyacrylamide gel and run at 4°C. Bands were visualized and quantified by phosphoimager analysis. Experiments with assembled WT and mutant Mre11 complexes were done accordingly using 5 nM DNA substrate.

Meiotic DSB formation

SK1 cells were cultured and genomic DNA was extracted as described [48]. For meiotic DSB detection, PstI digested genomic DNA was transferred on Hybond-XL membrane (Amersham Biotech) by alkaline transfer and meiotic DSBs at *HIS4-LEU2* were probed using a 1.5 kb EcoRI/BglII fragment of *pNKY291* [29].

Telomere Southern blot

Telomeres were detected by southern blot with PstI digested genomic DNAand a telomere specific probe (5′-TGTGGTGTGTGGGTGTGGTGT-3′) as described [49].

Sister chromatid recombination (SCR) and heteroallelic recombination

SCR was assessed as described [7]. DNA was purified from cells, XhoI/SpeI digested and analyzed by Southern blotting with a radiolabeled 0.218 kb *LEU2* probe (from 164–383). Southern blots, DNA labeling and quantification (Fuji FLA5000) were performed according to standard procedures [7]. The 1.4 kb and 2.4 kb fragments, arising as a result of HO cleavage, and the 4.7 kb specific for unequal SCR, were used for quantification of DSBs and SCR events, respectively and normalized to the total DNA per lane [31]. SCR experiments were repeated 2–3 times for each strain.

Heteroallelic mitotic recombination was assessed in diploid strains containing the *ade2-ISceI* and *ade2-n* heteroalleles [33,34]. 5–7 independent red colonies per genotype were re-plated on plates containing 7.5 μg ml^{-1} adenine and incubated for 9 (12) days at 30°C (23°C). White sectors within 200–500 red colonies were counted for each colonyplated.

NHEJ assays

For plasmid rejoining assays, cells were transformed with 400 ng of EcoRI or SacI linearized and in parallel with supercoiled *pRS313* and plated on plates lacking histidine. To monitor error-prone NHEJ at the *MAT l*ocus [35,50], cells were plated on galactose and glucose media and the efficiency of NHEJ was determined by the ratio of colonies grown on galactose versus glucose plates after 4 days incubation. NHEJ repair junctions were amplified from genomic DNA with primers flanking the HO site (YP017: CACATTAAATACCAACCCATCCG; YP028: GGAACAAGAGCAAGACGATGG) and sequenced with primer YP029 (GGATAGCTATACTGACAACATTCA). To measure NHEJ efficiencies after acute (2 or 4 hours) HO induction in galactose media, cells were collected and plated on glucose plates. Percentage cell survival was determined by the

number of colonies formed versus cells plated after 3–4 days incubation. To analyze NHEJ repair of the HO DSB by qPCR, HO was induced for 2 hours in galactose media and cells were harvested before (t=0) and after 1.5, 3 and 5 hours glucose addition (final concentration 2%). qPCR was performed as described elsewhere [51] with primers annealing to either side of the HO DSB (F: GGAATATGG GACTACTTCGCG; R: ACCAAAACCAGGGTTTATAAAATTATA) and normalized with PCRs for *PHO5, TUB2, ACT1*. NHEJ efficiencies were calculated as described [52].

Supplementary Material

Refer to Web version on PubMed Central for supplementary material.

Acknowledgments

MAIN REFERENCES

1. Stracker TH, Petrini JH. The MRE11 complex: starting from the ends. Nat Rev Mol Cell Biol. 2011; 12:90–103. [PubMed: 21252998]

2. Williams RS, Williams JS, Tainer JA. Mre11-Rad50-Nbs1 is a keystone complex connecting DNA repair machinery, double-strand break signaling, and the chromatin template. Biochem Cell Biol. 2007; 85:509–20. [PubMed: 17713585]

3. Paull TT, Gellert M. The 3′ to 5′ exonuclease activity of Mre 11 facilitates repair of DNA double-strand breaks. Mol Cell. 1998; 1:969–79. [PubMed: 9651580]

4. Bressan DA, Olivares HA, Nelms BE, Petrini JH. Alteration of N-terminal phosphoesterase signature motifs inactivates Saccharomyces cerevisiae Mre11. Genetics. 1998; 150:591–600. [PubMed: 9755192]

5. Bressan DA, Baxter BK, Petrini JH. The Mre11-Rad50-Xrs2 protein complex facilitates homologous recombination-based double-strand break repair in Saccharomyces cerevisiae. Mol Cell Biol. 1999; 19:7681–7. [PubMed: 10523656]

6. Moreau S, Ferguson JR, Symington LS. The nuclease activity of Mre11 is required for meiosis but not for mating type switching, end joining, or telomere maintenance. Mol Cell Biol. 1999; 19:556–66. [PubMed: 9858579]

7. Gonzalez-Barrera S, Cortes-Ledesma F, Wellinger RE, Aguilera A. Equal sister chromatid exchange is a major mechanism of double-strand break repair in yeast. Mol Cell. 2003; 11:1661–71. [PubMed: 12820977]

8. Hopfner KP, et al. The Rad50 zinc-hook is a structure joining Mre11 complexes in DNA recombination and repair. Nature. 2002; 418:562–6. [PubMed: 12152085]

9. Hopfner KP, Putnam CD, Tainer JA. DNA double-strand break repair from head to tail. Curr Opin Struct Biol. 2002; 12:115–22. [PubMed: 11839498]

10. Wiltzius JJ, Hohl M, Fleming JC, Petrini JH. The Rad50 hook domain is a critical determinant of Mre11 complex functions. Nat Struct Mol Biol. 2005; 12:403–7. [PubMed: 15852023]

11. Williams GJ, Lees-Miller SP, Tainer JA. Mre11-Rad50-Nbs1 conformations and the control of sensing, signaling, and effector responses at DNA double-strand breaks. DNA Repair (Amst). 2010; 9:1299–306. [PubMed: 21035407]

12. Williams RS, et al. Mre11 dimers coordinate DNA end bridging and nuclease processing in double-strand-break repair. Cell. 2008; 135:97–109. [PubMed: 18854158]

13. de Jager M, et al. Differential arrangements of conserved building blocks among homologs of the Rad50/Mre11 DNA repair protein complex. J Mol Biol. 2004; 339:937–49. [PubMed: 15165861]

14. Moreno-Herrero F, et al. Mesoscale conformational changes in the DNA-repair complex Rad50/Mre11/Nbs1 upon binding DNA. Nature. 2005; 437:440–3. [PubMed: 16163361]

15. Chen L, Trujillo K, Ramos W, Sung P, Tomkinson AE. Promotion of Dnl4-catalyzed DNA end-joining by the Rad50/Mre11/Xrs2 and Hdf1/Hdf2 complexes. Mol Cell. 2001; 8:1105–15. [PubMed: 11741545]

16. de Jager M, et al. Human Rad50/Mre11 is a flexible complex that can tether DNA ends. Mol Cell. 2001; 8:1129–35. [PubMed: 11741547]

17. Trujillo KM, et al. Yeast xrs2 binds DNA and helps target rad50 and mre11 to DNA ends. J Biol Chem. 2003; 278:48957–64. [PubMed: 14522986]

18. Chen L, et al. Effect of amino acid substitutions in the rad50 ATP binding domain on DNA double strand break repair in yeast. J Biol Chem. 2005; 280:2620–7. [PubMed: 15546877]

19. Costanzo V, Paull T, Gottesman M, Gautier J. Mre11 assembles linear DNA fragments into DNA damage signaling complexes. PLoS Biol. 2004; 2:E110. [PubMed: 15138496]

20. van der Linden E, Sanchez H, Kinoshita E, Kanaar R, Wyman C. RAD50 and NBS1 form a stable complex functional in DNA binding and tethering. Nucleic Acids Res. 2009; 37:1580–8. [PubMed: 19151086]

21. van Noort J, et al. The coiled-coil of the human Rad50 DNA repair protein contains specific segments of increased flexibility. Proc Natl Acad Sci U S A. 2003; 100:7581–6. [PubMed: 12805565]

22. Uhlmann F, Wernic D, Poupart MA, Koonin EV, Nasmyth K. Cleavage of cohesin by the CD clan protease separin triggers anaphase in yeast. Cell. 2000; 103:375–86. [PubMed: 11081625]

23. Anderson DE, Trujillo KM, Sung P, Erickson HP. Structure of the Rad50 x Mre11 DNA repair complex from Saccharomyces cerevisiae by electron microscopy. J Biol Chem. 2001; 276:37027–33. [PubMed: 11470800]

24. Hopfner KP, et al. Structural biochemistry and interaction architecture of the DNA double-strand break repair Mre11 nuclease and Rad50-ATPase. Cell. 2001; 105:473–85. [PubMed: 11371344]

25. Williams GJ, et al. ABC ATPase signature helices in Rad50 link nucleotide state to Mre11 interface for DNA repair. Nat Struct Mol Biol. 2011; 18:423–31. [PubMed: 21441914]

26. Lammens K, et al. The Mre11:Rad50 Structure Shows an ATP-Dependent Molecular Clamp in DNA Double-Strand Break Repair. Cell. 2011; 145:54–66. [PubMed: 21458667]

27. Lim HS, Kim JS, Park YB, Gwon GH, Cho Y. Crystal structure of the Mre11-Rad50-ATP{gamma}S complex: understanding the interplay between Mre11 and Rad50. Genes Dev. 2011

28. Hopfner KP, et al. Structural biology of Rad50 ATPase: ATP-driven conformational control in DNA double-strand break repair and the ABC-ATPase superfamily. Cell. 2000; 101:789–800. [PubMed: 10892749]

29. Keeney S, Kleckner N. Covalent protein-DNA complexes at the 5′ strand termini of meiosis-specific double-strand breaks in yeast. Proc Natl Acad Sci USA. 1995; 92:11274–11278. [PubMed: 7479978]

30. Kadyk LC, Hartwell LH. Sister chromatids are preferred over homologs as substrates for recombinational repair in *Saccharomyces cerevisiae*. Genetics. 1992; 132:387–402. [PubMed: 1427035]

31. Cortes-Ledesma F, Aguilera A. Double-strand breaks arising by replication through a nick are repaired by cohesin-dependent sister-chromatid exchange. EMBO Rep. 2006; 7:919–26. [PubMed: 16888651]

32. Ajimura M, Leem SH, Ogawa H. Identification of new genes required for meiotic recombination in Saccharomyces cerevisiae. Genetics. 1993; 133:51–66. [PubMed: 8417989]

33. Huang KN, Symington LS. Mutation of the gene encoding protein kinase C 1 stimulates mitotic recombination in Saccharomyces cerevisiae. Mol Cell Biol. 1994; 14:6039–45. [PubMed: 8065337]

34. Mozlin AM, Fung CW, Symington LS. Role of the Saccharomyces cerevisiae Rad51 paralogs in sister chromatid recombination. Genetics. 2008; 178:113–26. [PubMed: 18202362]

35. Moore JK, Haber JE. Cell cycle and genetic requirements of two pathways of nonhomologous end-joining repair of double-strand breaks in Saccharomyces cerevisiae. Mol Cell Biol. 1996; 16:2164–2173. [PubMed: 8628283]

36. Boulton SJ, Jackson SP. Components of the Ku-dependent non-homologous end-joining pathway are involved in telomeric length maintenance and telomeric silencing. Embo J. 1998; 17:1819–28. [PubMed: 9501103]

37. Lamarche BJ, Orazio NI, Weitzman MD. The MRN complex in double-strand break repair and telomere maintenance. FEBS Lett. 584:3682–95. [PubMed: 20655309]

38. Tseng SF, Gabriel A, Teng SC. Proofreading activity of DNA polymerase Pol2 mediates 3′-end processing during nonhomologous end joining in yeast. PLoS Genet. 2008; 4:e1000060. [PubMed: 18437220]

39. Hochwagen A, Tham WH, Brar GA, Amon A. The FK506 binding protein Fpr3 counteracts protein phosphatase 1 to maintain meiotic recombination checkpoint activity. Cell. 2005; 122:861–73. [PubMed: 16179256]

40. McVey M, Lee SE. MMEJ repair of double-strand breaks (director's cut): deleted sequences and alternative endings. Trends Genet. 2008; 24:529–38. [PubMed: 18809224]

41. Palmbos PL, Daley JM, Wilson TE. Mutations of the Yku80 C terminus and Xrs2 FHA domain specifically block yeast nonhomologous end joining. Mol Cell Biol. 2005; 25:10782–90. [PubMed: 16314503]

42. Matsuzaki K, Shinohara A, Shinohara M. Forkhead-associated domain of yeast Xrs2, a homolog of human Nbs1, promotes nonhomologous end joining through interaction with a ligase IV partner protein, Lif1. Genetics. 2008; 179:213–25. [PubMed: 18458108]

43. Makarova O, Kamberov E, Margolis B. Generation of deletion and point mutations with one primer in a single cloning step. Biotechniques. 2000; 29:970–2. [PubMed: 11084856]

44. Schiestl RH, Gietz RD. High efficiency transformation of intact yeast cells using single stranded nucleic acids as a carrier. Curr Genet. 1989; 16:339–46. [PubMed: 2692852]

45. Kim HS, et al. Functional interactions between Sae2 and the Mre11 complex. Genetics. 2008; 178:711–23. [PubMed: 18245357]

46. Trujillo KM, Sung P. DNA structure-specific nuclease activities in the Saccharomyces cerevisiae Rad50*Mre11 complex. J Biol Chem. 2001; 276:35458–64. [PubMed: 11454871]

47. Furuse M, et al. Distinct roles of two separable in vitro activities of yeast mre11 in mitotic and meiotic recombination. Embo J. 1998; 17:6412–25. [PubMed: 9799249]

48. Murakami H, Borde V, Nicolas A, Keeney S. Gel electrophoresis assays for analyzing DNA double-strand breaks in Saccharomyces cerevisiae at various spatial resolutions. Methods Mol Biol. 2009; 557:117–42. [PubMed: 19799180]

49. Chan SW, Chang J, Prescott J, Blackburn EH. Altering telomere structure allows telomerase to act in yeast lacking ATM kinases. Curr Biol. 2001; 11:1240–50. [PubMed: 11525738]

50. Sugawara N, Haber JE. Repair of DNA double strand breaks: in vivo biochemistry. Methods Enzymol. 2006; 408:416–29. [PubMed: 16793384]

51. Bryant GO, et al. Activator control of nucleosome occupancy in activation and repression of transcription. PLoS Biol. 2008; 6:2928–39. [PubMed: 19108605]

52. Shim EY, et al. RSC mobilizes nucleosomes to improve accessibility of repair machinery to the damaged chromatin. Mol Cell Biol. 2007; 27:1602–13. [PubMed: 17178837]
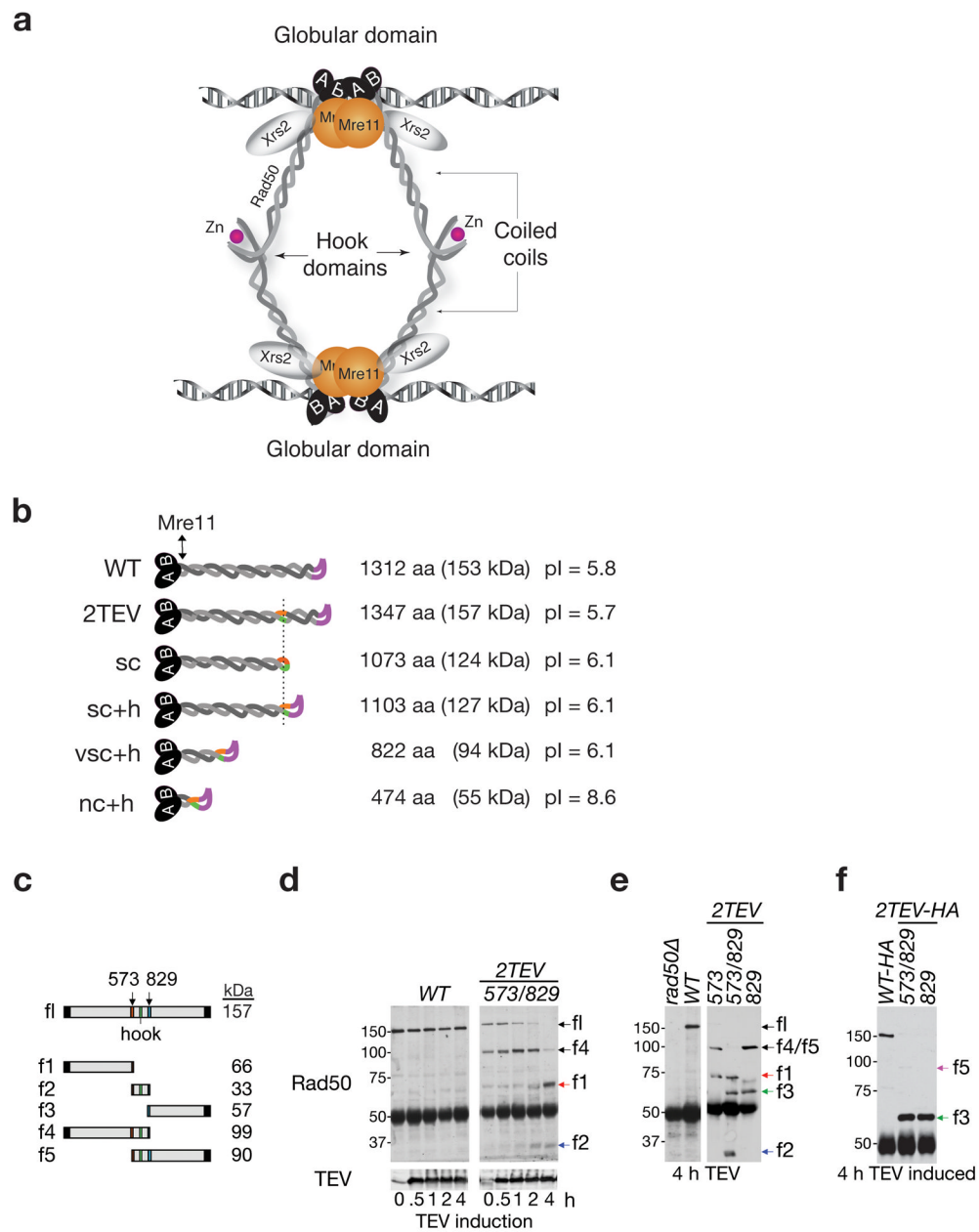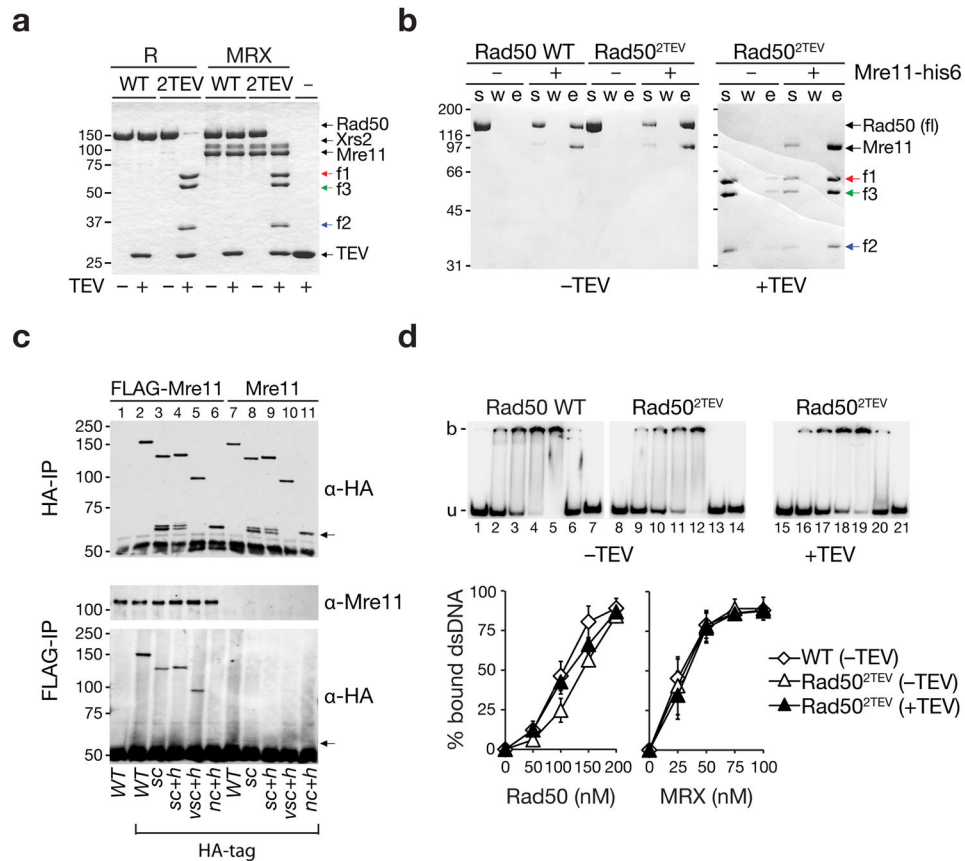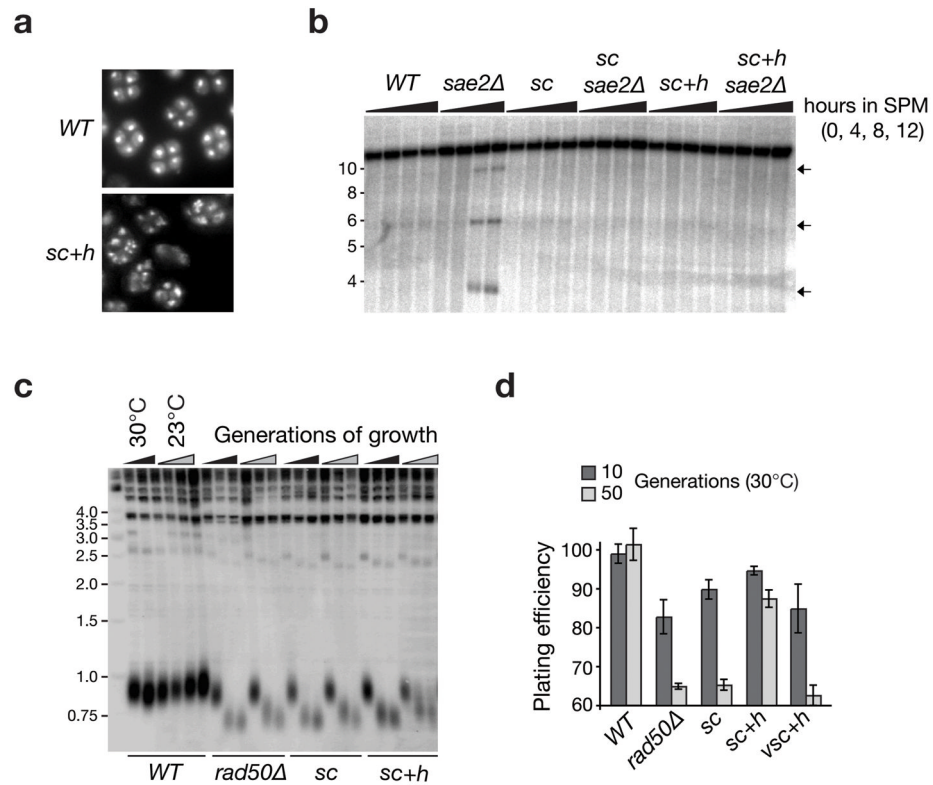
Figure 1.
Rad50 coiled coil mutants. (**a**) Mre11 complexes in the process of bridging sisters. (**b**) Rad50 coiled coil mutants created in this study. TEV protease recognition sites are highlighted in orange and green and the hook in magenta. The dashed line indicates that TEV protease cleavage of Rad50[2TEV], Rad50[sc] and Rad50[sc+h] results in almost identical Rad50 cleavage products lacking the hook domain. The Mre11 interacting interface of Rad50 proximal to the Rad50 ATPase core [25–27] is indicated. aa, amino acids; pI, isoelectric point. (**c**) Rad50[2TEV] primary protein structure with 2TEV recognition sequences at residues 573 and 829 on either side of the hook. The expected molecular weights of the protease cleavage fragments (f1–5) are indicated. (**d**) *In vivo* TEV protease induction results in proteolytic cleavage of the Rad50 hook domain in *rad50[2TEV]* cells. Rad50 WT (153kDa) and Rad50[2TEV] (157kDa) full length (fl) and Rad50[2TEV] cleavage products were visualized

by Rad50-immunoprecipitation (IP) and Rad50 western blot. Expression of the Myc-epitope tagged TEV protease was monitored in extracts by western blotting with Myc-antisera (bottom). (**e**) *In vitro* TEV cleavage of Rad50 WT and Rad50^{2TEV} proteins. Full length Rad50 was immunoprecipitated with Rad50 antisera, cleaved with recombinant TEV protease and analyzed by western blotting. (**f**) Rad50 pull down of 3xHA-tagged Rad50 proteins after TEV protease induction *in vivo*. Rad50^{2TEV} C-terminal cleavage fragments were detected by western blot with an anti-HA antibody. The 3xHA tag adds ~5 kDa to the molecular mass. Rad50-cleavage fragments in 1d-f are labeled as in Figure 1c.

Figure 2.
Mre11 complex integrity and DNA association is intact in absence of the hook and most of the coiled coil. (**a**) Coomassie stain of reconstituted Rad50^{2TEV}-containing Mre11 complexes with and without TEV cleavage. (**b**) TEV cleaved Rad50^{2TEV} interacts with Mre11. Indicated complexes containing His$_6$-Mre11 were captured with Ni-NTA agarose beads with and without TEV cleavage. Supernatant (s), wash (w), and SDS eluate (e) were analyzed by SDS-PAGE. The f2 hook fragment remained non-covalently associated following TEV cleavage under conditions used. (**c**) Mre11 complex integrity in Rad50 WT and *rad50^{coils}*. Rad50-HA tagged (lanes 2–11), FLAG-Mre11 (lanes 1–6) or untagged Mre11 (lanes 7–11) were immunoprecipitated and analyzed by Western blotting with the indicated antisera. Arrow refers to the expected migration level of the Rad50^{nc+h} protein. (**d**) DNA binding of Rad50^{2TEV} alone and in complex. Top: EMSA in presence of ATP with 0 (lanes 1, 8 and 15), 50 (lanes 2, 9 and 16), 100 (lanes 3, 10 and 17), 150 (lanes 4, 11 and 18) and 200 nM Rad50 (lanes 5, 12 and 19); untreated WT (left), untreated Rad50^{2TEV} (middle), and TEV treated Rad50^{2TEV} (right). Rad50 (200 nM) was incubated in binding buffer without ATP (lanes 6, 13 and 20) or treated with SDS and proteinase K (lanes 7, 14 and 21). Bound (b), unbound (u) DNA was separated under native conditions. Rad50 and Rad50^{2TEV} alone (bottom left) or in complex (bottom right). Representative gel pictures are shown in Supplementary Figure 1a.

Figure 3.
rad50 hook and coiled coil mutants are defective in meiotic DSB-formation and telomere maintenance. (**a**) Diploid SK1 *WT* and *rad50^{sc+h}* cells were cultivated in sporulation media for 2 days and Dapi-stained. (**b**) Meiotic DSB-formation at the *HIS4-LEU2* meiotic hotspot. Cells were cultivated for 0, 4, 8 and 12 hours in sporulation media (SPM) and meiotic DSB formation was detected by southern blot with a hotspot specific probe. Arrows refer to the migration levels of the two major Spo11-cleavage fragments (3.7 and 6.0 kb) and a minor one around 10 kb. (**c**) Telomere length after 0, 30 and 60 generations of growth at 30 or 23°C. Genomic DNA was digested with PstI and telomeres were visualized by southern blot using a telomere specific probe. (**d**) Plating efficiency after 10 and 50 generations of growth at 30°C.
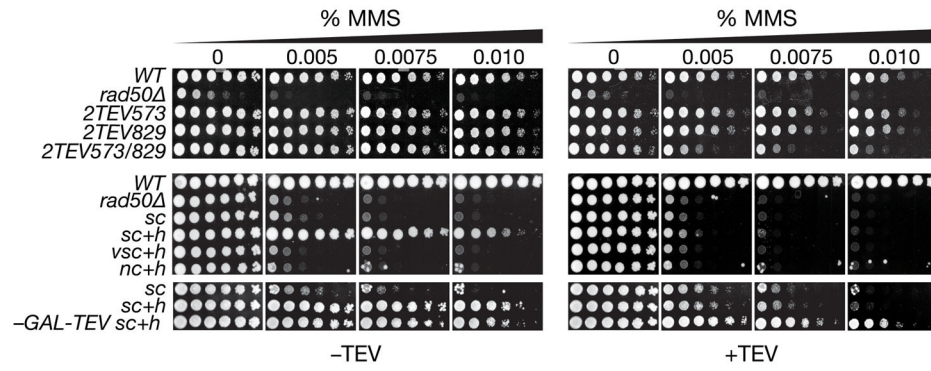
Figure 4.
The Rad50 hook and coiled coil domains are required for cell survival in presence of MMS. Cell survival on plates containing the indicated concentrations of MMS without (−TEV; glucose) or with TEV protease expression (+TEV; galactose). All strains contain the *TEV* expression cassette, except one labeled with "– *GAL-TEV*". Plates were incubated for 4 days at 30°C. MMS-sensitivity at different incubation temperatures (23°C and 37°C), as well as a quantitative assessment of the MMS sensitivity is given in Supplementary Figure 3a–c.

Figure 5.
Sister chromatid recombination (SCR) is promoted by the Rad50 hook and coiled coil domain. (**a**) *pRS316-TINV* SCR plasmid and products: unequal sister chromatid exchange (SCE) and intrachromatid recombination (ICR). The 4.7 kb band specific for SCE and the 2.9 kb band for SCE and ICR can be visualized after XhoI/SpeI digestion in southern blots using a *LEU2* probe. (**b**) Kinetics of DSB formation and repair. Top panel: HO induction for 0, 2, 4 and 6 hours without (−TEV; no *GAL-TEV*) or with TEV protease expression (+TEV). The ratio of the 4.7-kb band and the total plasmid was used to calculate SCE. Lower panel: HO induction over 24 hours (0, 3, 6, 9, 12 and 24 hours) without TEV expression. At 6 hours, SCR was not significantly different between $rad50^{sc}$ (0.9 ± 0.1%) and $rad50^{sc+h}$ (1.4 ± 0.1%; p >0.1). At 24 hours $rad50^{sc}$ (1.3% ± 0.03) and $rad50^{sc+h}$ (2.9± 0.5%) were significantly different (p<0.0002; two-tailed Wilcoxon rank sum test). (**c**) Assessment of spontaneous *ade2* heteroallelic mitotic recombination. Diploid *ade2-n/ade2-l-SceI, RAD50 WT* or *rad50* mutant colonies were re-plated on plates with limiting concentration of adenine. White sectors (*ADE2)* within red colonies (*ade2)* were scored. The percentage of colonies containing 0, 1–2, 3–4, >4 and >10 white sector(s) and the average numbers of sectors per colony is shown.

Figure 6.
NHEJ in *rad50coils*. (**a**) Plasmid-based NHEJ assays carried out as described in "Methods."
Ratios between *rad50sc+h* and *rad50Δ* were significantly different (EcoRI, p=0.036; SacI
p=0.024; two tailed t-test). (**b**) Survival frequency of strains with chronic HO induction.
Repair junctions were analyzed and the numbers of small insertions or deletions are
indicated. Sequences are given in Supplementary Figure 5a. (**c**) Top: Cell survival upon
chronic HO induction without or with concomitant TEV expression. Bottom: Repair
junctions of *rad50^2TEV* survivors (without or with *TEV*) were analyzed. Sequences are listed
in Supplementary Figure 5c. (**d**) NHEJ repair kinetics following acute (2 hours) HO
induction were determined by qPCR. Cells were cultivated for another 1.5, 3 or 5 hours in
glucose media following HO induction and repair monitored with primers flanking the HO
site. (**e**) Cell survival and NHEJ repair events after acute HO DSB induction. Top: Cell
survival after 2 hours HO induction. qPCR demonstrated that more than 94% of the HO
induced cells plated contained an HO DSB (data not shown). Bottom: The numbers of
imprecise NHEJ repair events versus the total numbers of HO junctions sequenced is given.
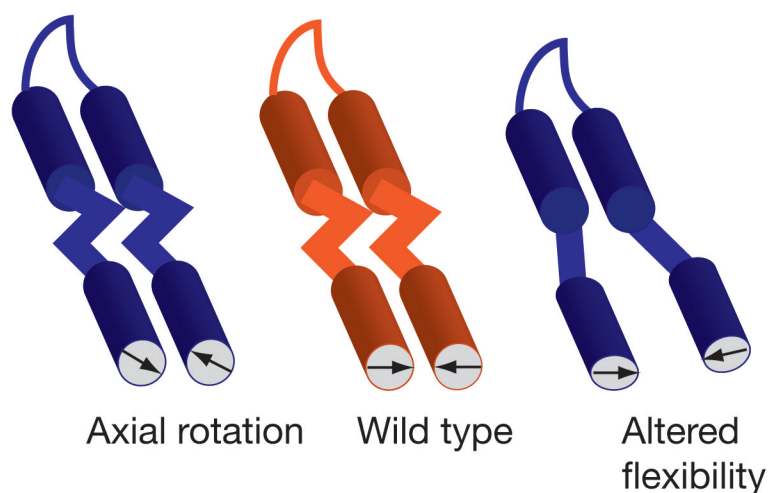*rad50^nc+h* was assessed only in 1 experiment.

Axial rotation   Wild type   Altered flexibility

Figure 7.
Distal domain alterations and potential effects on the globular domain. Depicted are the two lobes of the heterotetrameric Mre11 complex globular DNA binding domain, from which two extended coiled coils protrude. The globular domain orientation is indicated by arrows. Zigzag lines indicate flexible regions. To account for the effects of $rad50^{coils}$ and $rad50^{2TEV}$ on NHEJ, we propose that coiled coil shortening and TEV-mediated hook cleavage perturb the coils in two non-exclusive manners. Axial rotation of the coils, causing misalignment of the globular domain is envisioned in both $rad50^{coils}$ and $rad50^{2TEV}$, and altered flexibility is envisioned in $rad50^{coils}$ mutants. In these scenarios, axial rotations may cause distortion of the globular domain that alters the disposition of DNA ends held within it. Alterations in coiled coil flexibility may disrupt the juxtaposition of two ends. Both outcomes have the potential to alter the efficiency and junctional sequences of NHEJ.